Numerical Simulation of High-Power Virtual-Cathode Reflex Triode Driven by Repetitive Short Pulse Electron Gun

Ivailo G. Yovchev, Ivan P. Spassovsky, Nikolai A. Nikolov, Dimitar P. Dimitrov, Giovanni Messina, Pantaleo Raimondi, Joaquim J. Barroso, and Rafael A. Corrêa

***Abstract*— A virtual-cathode reflex triode is investigated by numerical simulations. A trapezoidal in shape voltage pulse with an amplitude of 300 kV is applied to the solid cathode of the device to drive the cathode negative. The electron beam-to-microwave power conversion efficiency ϵ, calculated for the pulse flat top with a duration $\tau_{ft} = 1.2$ ns is approximately the same (about 1.5–2%) as well as for a long flat top ($\tau_{ft} = 4$ ns). The simulations show a 10–15% increase of ϵ at τ_{ft} shortening to 0.6 ns. However, this occurs when the anode mesh transparency is high (80–90%). Considerable enhancement of the efficiency (about four times) for $\tau_{ft} = 0.6$ ns has been calculated if the cathode side surface is brought near to the anode tube (from $\approx$0.5% at cathode radius $R_c = 1.6$ cm to $\approx$2% at $R_c = 3.8$ cm). The obtained results would find an application for the design of virtual-cathode reflex triode devices driven by a short pulse and high repetition rate electron gun.**

I. Introduction

IN THE PAST few years several laboratories and research centers concentrated their efforts on development and construction of new low-cost, high repetition rate, and flexible electron guns for different applications in medicine, material treatment, spectroscopy, radars, etc. Such a machine has been already designed and constructed at ENEA (Italy) to power a free-electron laser (FEL) operating in the far infrared region. However, it can be used successfully to drive various microwave sources. In this paper numerical simulations, which have been performed for the future foil-diode vircator experiment, carried out at the ENEA gun are reported.

II. Electron Gun Design

A schematic diagram of the machine is shown in Fig. 1. The compactness required for the accelerator has brought the constructors to develop a pulser operating at high repetition rate with very short pulse duration. As can be seen from the principal scheme, the electron gun is simply composed of five main components. First, a 20-kV power supply charges a capacitor bank C_0 up to 20 kV, which plays the role of a primary energy storage reservoir. Next, discharge by the thyratron generates a 1-μs long pulse. Usually, in the conventional pulse power conditioning circuits and systems, the output pulse energy is transferred from the power supply to an intermediate energy storage device through a conventional switch. However, the most repetitive machines use a resonant charge or resonant energy transfer circuit. Such an idea has been realized with the ENEA design, where a six-stage parallel magnetic pulse compressor, referred to here as a pulse compressing system (PCS), was constructed. Its main advantage is the voltage level shift provided by the transformers. The

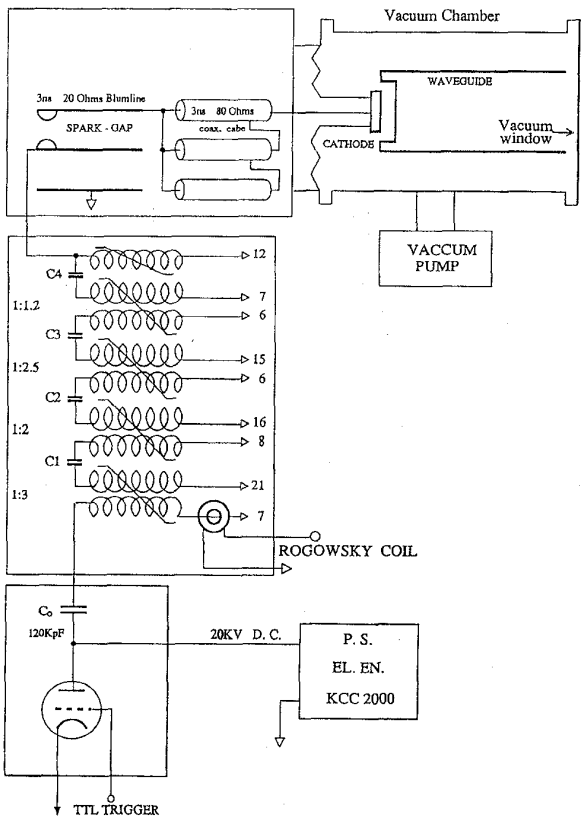

Fig. 1. Schematic diagram of short pulse high-frequency repetition electron gun.

Manuscript received September 2, 1995; revised February 22, 1996.

I. G. Yovchev, I. P. Spassovsky, N. A. Nikolov, and D. P. Dimitrov are with the Faculty of Physics, Sofia University, Sofia 1126 Bulgaria (e-mail: kosta@phys.uni-sofia.bg).

G. Messina is with ENEA, INN-FIS-LAC, 00044 Frascati, Rome, Italy.

P. Raimondi is with the Stanford Linear Accelerator Center, Stanford, CA 94305 USA.

J. J. Barroso and R. A. Corrêa are with INPE, São Jose dos Campos 12227-970 São Paulo, Brazil.

Publisher Item Identifier S 0093-3813(96)05243-5.

full configuration of the PCS reduces the pulse down to 30 ns and rises the voltage up to 350 kV at the final condenser of the compressor (the double pulse forming line, or PFL) with energy transfer efficiency of about 70%. The line is filled with distilled water in order to minimize the size of the system. Its length is calculated so that it forms a 3-ns output pulse. Since the gun is designed to drive an FEL, the pulse is transformed additionally using a transmission line transformer (TLT). It consists of three coaxial 80-Ω cables charged in parallel from the Blumline side and discharged in series on the diode load. If the diode is mismatched the voltage pulse could raise up to 1.8 MV. In our simulations we used a reduced scheme without TLT, i.e., the self-triggering line directly powers the diode. This gives the possibility of getting a higher beam current at lower voltages. As we mentioned before, by generating a short pulse we are able to minimize the physical size of the machine. Moreover, an important problem with foil–anode diodes, which we use, is the diode closure. It comes from the plasma effect produced by the electron collisions drifting into the gap. The effective closure of the gap decreases the impedance, causing runaway electron current or collapsing the voltage on a time scale of 50 to 100 ns. For our 3-ns pulse we can decrease considerably the anode–cathode gap. In addition, it has been experimentally demonstrated [1] that for the pulse in the vicinity of few nanoseconds duration a gradient of 900 MV/m can be held without an electric breakdown occuring. Hence, we might use this advantage to construct an optimal diode configuration, where the distance between the side cathode surface and the anode tube is determined only by the electric breakdown limitation.

III. Simulations with an Anode Foil Model

It is the purpose of this paper to report a numerical investigation concerned with the optimal values of the solid cathode radius and pulse flat top duration with respect to the microwave radiation power and beam-to-microwave energy conversion efficiency for the future vircator experiment. The efficiencies calculated for the flat tops of the short pulse, produced by the ENEA gun, and of a long pulse are compared. Simulations are also performed for studying the influence of the mesh transparency.

The short pulses generated by the gun described above are approximately trapezoidal in shape with rise, duration, and fall times 0.8, 1.2, and 1 ns, respectively. In all simulations considered below, the rise time of the voltage pulse is fixed at 0.8 ns.

An outline of the modeled axisymmetric system is shown in Fig. 2. The electron beam is formed in a foil diode with a 44-mm-radius anode tube. The electrons are generated by an explosive plasma emission from a solid cathode. A guiding magnetic field is absent. Beyond the anode foil positioned at a distance of $d = 6$ mm from the cathode front surface, the electrons propagate in an output drift tube (output waveguide) with a radius of $R_w = 40$ mm. Both the anode tube and the output waveguide including the foil are grounded.

The program KARAT [2] was used in numerical simulations of the described system. The code is fully relativistic, electromagnetic, and 2-1/2 dimensional—two spatial dependencies (r, z) and three velocity components in a cylindrical coordinate frame, based on the particle-in-cell method.

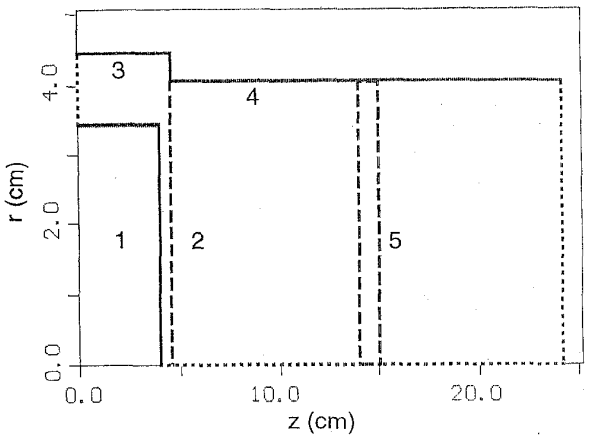

Fig. 2. Outline of the modeled system: 1) cathode, 2) anode foil, 3) anode tube, 4) waveguide, 5) electron absorber.

The first simulation was performed for a cathode radius of $R_c = 3.4$ cm. A 300-kV transverse electromagnetic (TEM) wave is input from the left-hand boundary of the modeled system, which drives the cathode negative. The rise and the duration time of the pulse are 0.8 and 6.2 ns, respectively. Since the pulse fall time is not important for the presented investigations it is not included in the simulations. We suppose also that a relatively low field (a field emission threshold of 20 kV/cm) causes space–charge limited emission from the front surface of the cold cathode toward the anode foil. On the other hand, the electron emission from the cathode side surface is neglected. These two suppositions are realistic enough if the front surface is covered with velvet in a real experiment [3] and the side surface is well polished so that the field emission threshold would be increased above $5 \cdot 10^5$ V/cm (considerably lower than the values of the gradient, which can be held by the metal surfaces at short pulses).

The anode foil was modeled as a perfect, infinitesimally thin conductor. The energy loss and the angle scattering of the electrons as they traverse through the foil were neglected. To stop the particles that would get to the points of RF field and power monitoring, an electron absorber (a dielectric region with a dielectric constant $\epsilon_r = 1$) is placed.

The computations show that at the moment of time $t \approx 0.6$ ns a virtual cathode (VC) is formed inside the waveguide at a distance from the anode foil approximately equal to d. After the VC formation, a microwave emission starts. The axial component of its Poynting vector $\Pi_z = E_r H_\varphi$ (E_r and H_φ are the radial and the azimuthal components of the RF electric and magnetic fields, respectively) was monitored near the right-hand boundary of the simulated region. In Fig. 3 a time history of Π_z at a point with coordinates $r = 3.5$ cm, $z = 22$ cm is depicted. It is clearly seen that Π_z has a maximum at the beginning of the microwave pulse. This behavior of Π_z leads to the conclusion that the microwave production efficiency ϵ would be higher if the flat top of the TEM pulse is short (less than 1 ns).

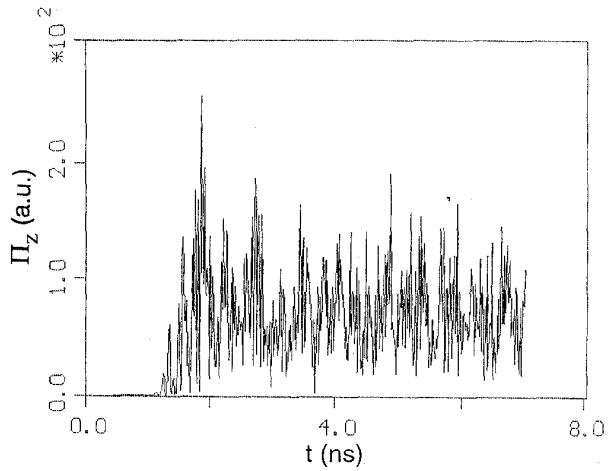

Fig. 3. Time history of the Poynting vector z-component in a point $r = 3.5$ cm, $z = 22$ cm.

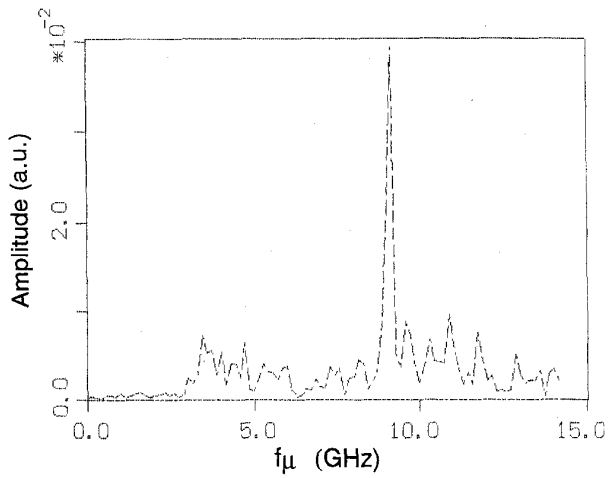

Fig. 4. Fourier transform of the azimuthal RF magnetic field in a point $r = 3.5$ cm, $z = 22$ cm.

For a 300-keV 3.4-cm radius solid electron beam, propagating in a 4-cm radius waveguide, the space–charge-limiting current is $I_{scl} = 2.8$ kA [4]. It was determined in the simulation that the average current I_c emitted by the cathode in the TEM pulse flat top is 24.1 kA. Thus, the ratio $I_c/I_{scl} \approx 9$. At large values of I_c/I_{scl}, the predominant source of the microwave radiation is the electron bunches, oscillating in the potential well between the real and the virtual cathodes [5].

To get an additional confirmation of the microwave source, we follow the method, reported in [6], where the azimuthal component of the RF magnetic field H_φ is monitored at the right-hand boundary (here in the point mentioned above: $r = 3.5$ cm, $z = 22$ cm), and the axial current I_{ax} is monitored at the anode foil. In Figs. 4 and 5 the Fourier transforms of H_φ and I_{ax}, respectively, are presented. Evidently, the H_φ peak coincides in frequency with the peak of I_{ax} ($\approx$9 GHz), which indicates that the main source of microwave radiation is the reflected electrons, oscillating between the real and the virtual cathodes.

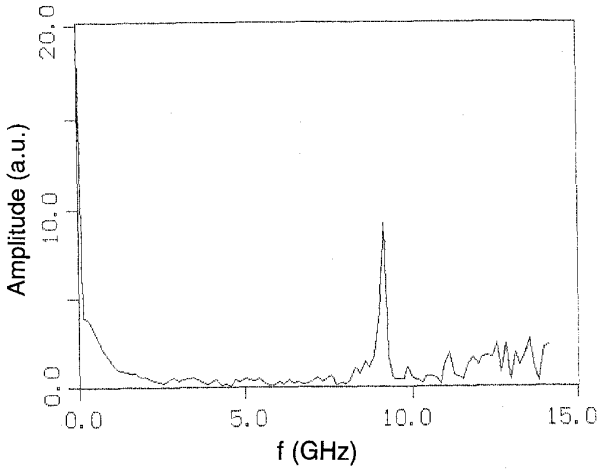

Fig. 5. Fourier transform of the beam current through the anode foil.

The frequency f_μ, corresponding to the maximum amplitude in the H_φ Fourier transform ($\approx$9 GHz) is higher than the TM_{01} and TM_{02} cutoff frequencies for a 4-cm radius waveguide (2.87 and 6.59 GHz, respectively) but lower than the TM_{03} cutoff frequency (10.34 GHz). Consequently, the dominant modes excited in the waveguide are TM_{01} and TM_{02}. However, the average power in these modes has not been determined separately. Instead, the output power of the microwave radiation was calculated by integration of Π_z over the waveguide cross section near the end of the simulated region. The output power P, determined at $z = 22$ cm and averaged over the time range (1.5, 2.2) ns is $\approx$130 MW. From 2.2 to 2.9 ns, P is approximately 80 MW. The decrease of P is considerable and is closely connected with the process of electron bunching.

We determine approximately at $R_c = 3.4$ cm the time τ of microwave pulse propagation from the VC region (with a coordinate $z_1 \approx 5$ cm) to the cross section of P monitoring ($z_2 = 22$ cm) using the relation [3]

$$(k_z c)^2 = \omega_\mu^2 - (\kappa_{0n} c/R_w)^2. \tag{1}$$

Here, $\omega_\mu = 2\pi f_\mu$; k_z, c, and κ_{0n} are the longitudinal wavenumber, the speed of light, and the zeroes associated with the zero-order Bessel function, J_0. From (1), taking into account that $f_\mu \approx 9$ GHz and assuming that the dominant mode excited in the waveguide is TM_{02}, the value of k_z can be determined as $k_z = 1.27$ cm^{-1}. Applying successively the formulas for the phase v_ϕ and the group v_g velocities ($v_\phi = \omega_\mu/k_z$, $v_g = c^2/v_\phi$), it is obtained that $v_g \approx 2 \cdot 10^{10}$ cm/s. Therefore, the time for microwave pulse propagation from z_1 to z_2 is $\tau_1 \approx 0.85$ ns. Using the same procedure and assuming that the dominant mode is TM_{01}, τ is evaluated as $\tau_2 \approx 0.63$ ns. For the value of τ it is reasonable to use the average of τ_1 and τ_2, $\tau \approx 0.75$ ns. Consequently, P in the time range (1.5, 2.2) ns results from the radiation of the electron bunches between approximately 0.7 and 1.4 ns. Similarly, P in the range (2.2, 2.9) ns results from the same process between 1.4 and 2.1 ns. In Figs. 6 and 7, the Fourier transform of the current through the foil in the time ranges (0.7, 1.4) and (1.4,

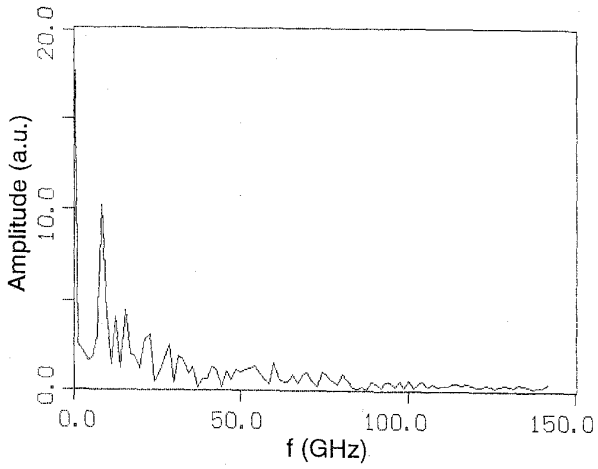

Fig. 6. Fourier transform of the beam current through the anode foil for time range (0.7, 1.4) ns at $R_c = 3.4$ cm.

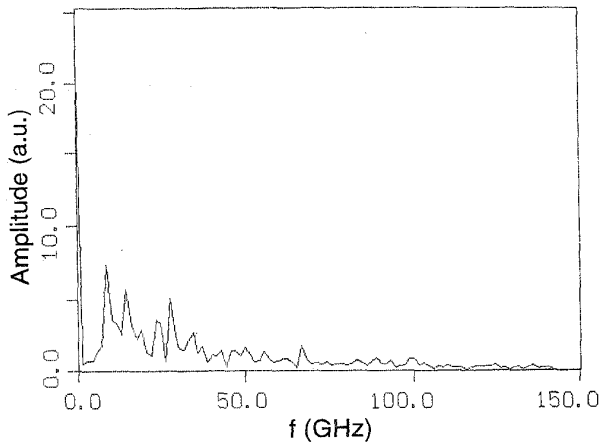

Fig. 7. Fourier transform of the beam current through the anode foil for time range (1.4, 2.1) ns at $R_c = 3.4$ cm.

2.1) ns, respectively, are shown. The peak at $f \approx 9$ GHz in Fig. 6 corresponds to a single bunch of electrons oscillating between the real and the virtual cathodes. As can be seen from Fig. 7, the peak at $f \approx 9$ GHz decreases and a second peak at $f \approx 15$ GHz appears. The second peak is a result of a new electron bunch formation with a higher transit frequency ω. The reason for the split of the reflected electrons roughly into two bunches with different transit frequencies is a two-stream instability [5]. The streaming instability leads to an angular divergence increase of part of the electrons and hence to their transverse kinetic energy enhancement at the expense of their longitudinal kinetic energy E_k. The transit frequency of these electrons becomes higher because $\partial\omega/\partial E_k < 0$ [7], and they form a new bunch. This new bunch is less efficient with respect to the microwave generation, since it is deflected quickly to the walls before a significant amount of microwave energy extracts from it [8]. For that reason, P in the time range (1.5, 2.2) ns is higher than P in the range (2.2, 2.9) ns.

In Table I the microwave production efficiency ϵ is given at $R_c = 3.4$ cm, calculated for the pulse flat top, as a function

TABLE I
CALCULATED EFFICIENCY ϵ AS A FUNCTION OF THE PULSE FLAT TOP DURATION $\tau_{ft} \in (0.1, 1.2)$ ns

τ_{ft} (ns)	0.1	0.2	0.3	0.4	0.5	0.6	0.7	0.8	0.9	1.0	1.1	1.2
ε (%)	1.94	1.83	2.05	1.97	1.80	1.75	1.78	1.69	1.71	1.65	1.61	1.53

TABLE II
DEFINED EFFICIENCIES AND CORRESPONDING TIME RANGES TO WHICH THEY REFER. THE MOMENTS OF TIME $t = 0$ AND $t = 0.8$ ns COINCIDE WITH THE BEGINNINGS OF THE TEM PULSE RISE AND TEM PULSE FLAT TOP, RESPECTIVELY

Efficiency	ε_f	ε_s	ε_{sh}	ε_l
Time range (ns)	(0.8, 1.4)	(1.4, 2.0)	(0.8, 2.0)	(0.8, 4.8)

of its duration τ_{ft}, changing from 0.1 to 1.2 ns, with a step of 0.1 ns. The efficiency ϵ is defined as a ratio $P/(UI_c)$. Here P is the output power of microwave radiation averaged over the time range (0.8, 0.8+τ_{ft}) ns and $U \approx 300$ kV is the mean diode voltage at the TEM pulse flat top.

After the pulse rise time, both I_c and U perform small-amplitude oscillations. The mean values of I_c for any time range with a duration of 0.1 ns from the pulse flat top differ no more than 5–6% from each other. The differences between the I_c values become insignificant if the averaging is performed over longer ranges (with durations of 0.5–0.6 ns). The same is valid for U. In this and in the following simulations I_c and U are the mean values of the cathode current and the diode voltage, respectively, for the first 4 ns of the flat top. The choice of such a time range is connected with the long pulse duration, discussed below.

From Table I a tendency toward a decrease (although not smooth) of ϵ with τ_{ft} increasing is obvious. The detailed study of $\epsilon(\tau_{ft})$ dependence when $\tau_{ft} \in (0.1, 1.2)$ ns is of no importance for the planned experiments, since at present $\tau_{ft} = 1.2$ ns. However, this dependence shows that the changes of the ENEA gun construction leading to a pulse flat top shortening below 1.2 ns would have a favorable effect on the vircator efficiency, at least for $R_c = 3.4$ cm.

Of more importance for the present stage is to compare the microwave production efficiencies for short (with $\tau_{ft} = 1.2$ ns) and long pulses. As an analogue of a long pulse, a pulse with a flat top duration of 4 ns was taken, since the simulation shows that the changes of the efficiency are negligible at longer τ_{ft} (5 or 6 ns).

The following efficiencies can be defined: ϵ_f, ϵ_s, ϵ_{sh}, and ϵ_l. They refer to different parts (time ranges) of the pulse flat top (see Table II) and are calculated as ratios $P/(UI_c)$. Here P is the output power of microwave radiation averaged over the corresponding time ranges given in Table II.

It is clear from Table II that ϵ_{sh} and ϵ_l are calculated for flat tops with durations $\tau_{ft} = 1.2$ ns and $\tau_{ft} = 4$ ns, respectively. They serve for comparing of the efficiencies of the short and long pulses. The other two quantities, ϵ_f and ϵ_s, refer to the first and second halves, respectively, of the short pulse flat top. By comparison of their values, we can understand whether it is necessary to make efforts for τ_{ft} shortening below 1.2 ns at varying R_c. For the same purpose, however, ϵ_f could be compared not with ϵ_s but with ϵ_{sh}, and consequently it is

TABLE III
SUMMARY OF SIMULATION RESULTS FOR THE ANODE FOIL MODEL

R_c(cm)	I_c (kA)	ε_f (%)	ε_s (%)	ε_{sh} (%)	ε_l (%)	$\varepsilon_f/\varepsilon_l$
1.6	6.6	0.48	1.09	0.78	1.20	0.40
2.0	8.4	1.04	1.55	1.30	1.48	0.70
2.2	9.6	1.33	1.85	1.59	1.62	0.82
2.4	10.6	1.53	1.56	1.55	1.31	1.17
2.6	12.3	1.42	1.43	1.43	1.45	0.98
2.8	14.1	1.75	1.27	1.51	1.44	1.22
3.0	16.5	1.50	1.30	1.38	1.35	1.11
3.2	19.9	1.81	1.28	1.50	1.51	1.20
3.3	21.2	1.78	1.38	1.55	1.53	1.16
3.4	24.1	1.75	1.30	1.53	1.42	1.23
3.5	26.8	1.89	1.51	1.70	1.61	1.17
3.6	30.0	1.68	1.41	1.54	1.46	1.15
3.7	33.6	1.70	1.06	1.38	1.42	1.20
3.8	38.6	1.92	1.23	1.58	1.38	1.39

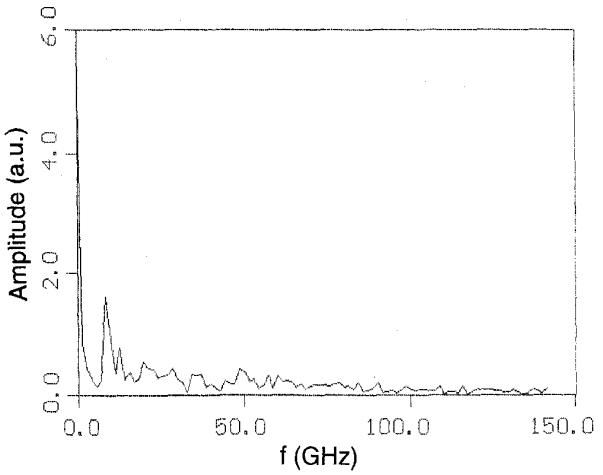

Fig. 8. Fourier transform of the beam current through the anode foil for time range (0.7, 1.4) ns at $R_c = 1.6$ cm.

not obligatory to define ϵ_s. Moreover, the efficiency for the second half of the short pulse flat top can be easily found using the obvious relation: $\epsilon_{sh} = (\epsilon_f + \epsilon_s)/2$. Nevertheless, we introduce ϵ_s for completeness. The duration of the time range, to which ϵ_f refers, is chosen to be 0.6 ns for definiteness and for symmetry (in this way the short pulse flat top is divided into two equal parts).

The value of ϵ_l, determined in the first simulation, is 1.42%. From Table I it can be seen that $\epsilon_f = \epsilon(0.6 \text{ ns}) = 1.75\%$ and $\epsilon_{sh} = \epsilon(1.2 \text{ ns}) = 1.53\%$. By use of the relation $\epsilon_{sh} = (\epsilon_f + \epsilon_s)/2$, it is obtained that $\epsilon_s = 1.31\%$. The following conclusions from the simulation for $R_c = 3.4$ cm in terms of the defined efficiencies can be drawn: 1) ϵ_f is considerably higher than $\epsilon_s (\epsilon_f/\epsilon_s = 1.34)$. Hence, as was mentioned above, the shortening of the pulse flat top below 1.2 ns is reasonable. 2) ϵ_f is above 20% larger than $\epsilon_l (\epsilon_f/\epsilon_l = 1.23)$. 3) ϵ_{sh} is a little greater in comparison with $\epsilon_l (\epsilon_{sh}/\epsilon_l = 1.08)$.

A series of simulations was performed to check whether the upper relations (inequalities) between the defined efficiencies [calculated again as ratios $P/(UI_c)$] remain valid for other R_c values. The results are presented in Table III. When $R_c > 3.4$ cm, a possibility of an electric breakdown between the cathode side surface and the anode tube exists. As was stated above, the metal surfaces can hold a gradient of up to 900 MV/m for the extremely short pulses, as ours. The simulated reflex triode configuration has not been investigated experimentally, and we are not sure that the electric breakdown would not occur in a real experiment. However, it is interesting to calculate the efficiencies if $R_c > 3.4$ cm. It is seen in Table III that at larger R_c ($\geq$ 2.8 cm), inequalities similar to those for $R_c = 3.4$ cm are fulfilled. On the other hand, inequalities 1 to 3 change to the opposite for smaller cathode radii (from 1.6 to 2.2 cm). In a sense, the two R_c values (2.4 and 2.6 cm) represent a transition region between larger and smaller radii. For instance, at $R_c = 2.4$ cm, $\epsilon_f < \epsilon_s$; however, $\epsilon_f > \epsilon_l$, i.e., the inequalities' signs are mixed. It is clear that the shortening of τ_{ft} below 1.2 ns is reasonable only for $R_c \geq 2.8$ cm.

From Table III, the following important conclusions about the efficiencies at greater radii can be made: 1) ϵ_f is ≈ 4 times larger than ϵ_f for $R_c = 1.6$ cm; 2) ϵ_{sh} is ≈ 2 times larger than ϵ_{sh} for $R_c = 1.6$ cm; 3) ϵ_l is a little bit larger than ϵ_l for $R_c = 1.6$ cm. Therefore, to improve the efficiency at short pulses (with a duration of their flat top from 0.6 to 1.2 ns) it is necessary to put the cathode side surface close to the anode tube wall. Indeed, the greatest values of P (above 100 MW) are calculated for large radii (≥ 3.2 cm) and for pulse flat top duration $\tau_{ft} = 0.6$ ns, at which the cathode currents I_c and the efficiencies ϵ_f are maximum.

The transition from $\epsilon_f > \epsilon_s$ at larger R_c to $\epsilon_f < \epsilon_s$ at smaller R_c can be qualitatively explained. It must be noted that with varying R_c, the frequency of the microwave radiation with maximum amplitude in the Fourier transform slightly changes, but it remains lower than 10.34 GHz. Thus, the dominant modes excited in the waveguide are again TM_{01} and TM_{02}, as in the case of $R_c = 3.4$ cm. The electron bunching is performed in the axial electric field E_z of TM_{0n} modes. Since the maximum of E_z for the TM_{01} mode is at the waveguide axis ($r = 0$), this mode would be excited with an efficiency almost independent of the cathode radius. Hence, the efficiency ϵ_f in the first 0.6 ns of the pulse flat top mainly depends on the extent to which the mode TM_{02} is excited in this time range. At $r = 0$, where the first E_z maximum of TM_{02} appears, the current density is quite small because of a strong potential depression. Therefore, the mode TM_{02} could not be excited efficiently by the electrons emitted in the region surrounding $r = 0$.

The second axial electric field maximum of TM_{02} is at $r \approx 2.8$ cm. If $R_c \geq 2.8$ cm (greater radii), most of the beam is launched around the second E_z maximum, and hence the electron bunches are quickly formed. This leads to a high-power microwave radiation at the beginning of the pulse flat top. In the case of smaller radii ($R_c \leq 2.2$ cm) most of the current is emitted near the minimum of the TM_{02} axial electric field ($r \approx 1.75$ cm). Therefore, the bunching is performed more slowly in comparison with the case of larger radii. In Figs. 8 and 9, the Fourier transform of the current through the foil at $R_c = 1.6$ cm for the time ranges (0.7, 1.4) and (1.4, 2.1) ns are shown, respectively. The amplitude peak at $f \approx 9$ GHz in Fig. 8 is lower than the same peak in Fig. 9, which is evidence for the bunch enhancement with time. This explains

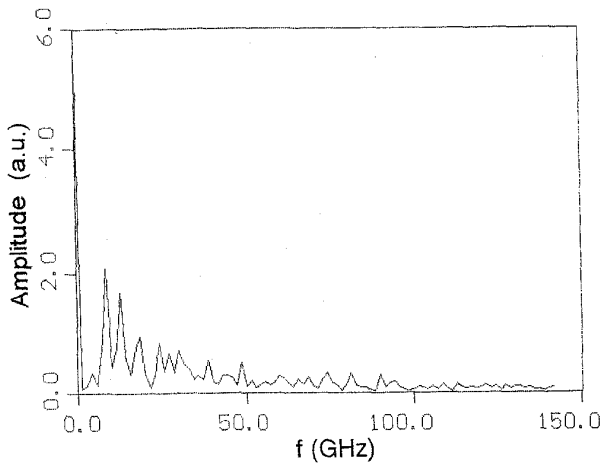

Fig. 9. Fourier transform of the beam current through the anode foil for time range (1.4, 2.1) ns at $R_c = 1.6$ cm.

the inequality $\epsilon_f < \epsilon_s$ at smaller radii. Again as a result of a two-stream instability, a second bunch at $f \approx 14$ GHz forms in the time range (1.4, 2.1) ns; see Fig. 9.

Within the framework of the qualitative considerations presented, a smooth transition from $\epsilon_f > \epsilon_l$ to $\epsilon_f < \epsilon_l$ would be expected when R_c decreases. However, Table III shows that at $R_c = 2.6$ cm, $\epsilon_f \approx \epsilon_l$, while at $R_c = 2.4$ cm and $R_c = 2.8$ cm, $\epsilon_f > \epsilon_l$. Therefore, these qualitative considerations explain only the general tendency, but not the details of the $\epsilon_f/\epsilon_l(R_c)$ dependence.

IV. Simulations with an Anode Mesh Model

The model of the infinitesimally thin foil was used to obtain a rough estimate for the efficiencies of the short pulses at different cathode radii. However, it is clear that this model is not realistic for a high repetition rate machine, because the thin foil would melt. On the other hand, at a thicker foil the microwave radiation power dramatically decreases, since the electrons suffer a velocity scattering [8]. That is why a mesh instead of a foil was used in the further, more realistic simulations. The model of the mesh is very simple. The mesh with a transparency of $q\%$ is again a perfect infinitesimally thin conductor. Each electron may be absorbed (and then removed from the calculations) with a probability $A = (100 - q)\%$ at each transit through the mesh. The probability of absorption A does not depend on the electron energy and the direction of the electron velocity.

With the described model of the mesh, two series of simulations were performed, varying A. The aims are to check whether at $A \neq 0$ the inequality $\epsilon_f > \epsilon_l$ holds and to compare ϵ_{sh} with ϵ_l. The expectation is that the ratio ϵ_f/ϵ_l would decrease with the increase in A. This determines the choice of the R_c values (3.4 and 3.8 cm) in the following simulations since for the mentioned values the ratios ϵ_f/ϵ_l are greatest at $A = 0$. The results for $R_c = 3.4$ cm and $R_c = 3.8$ cm are presented in Tables IV and V, respectively. In the first row of both tables, results of the former simulations when $A = 0$ are presented for comparison. In the third column of Table IV and Table V are given the currents in the drift tube I_{dt}, obtained according to the relation $I_{dt} = (1 - A)I_c$. The efficiencies were calculated as ratios $P/(UI_{dt})$.

TABLE IV
Summary of Simulations for the Anode Mesh Model at $R_c = 3.4$ cm

A (%)	I_c (kA)	I_{dt} (kA)	ε_f (%)	ε_s (%)	ε_{sh} (%)	ε_l (%)	$\varepsilon_f/\varepsilon_l$
0	24.1	24.1	1.75	1.30	1.53	1.42	1.23
5	25.3	24.0	1.87	1.18	1.53	1.65	1.13
10	26.2	23.6	2.10	1.77	1.93	1.83	1.15
15	26.8	22.8	1.64	1.48	1.56	1.66	0.99
20	27.3	21.8	1.80	1.60	1.70	1.81	0.99
40	28.5	17.1	0.92	2.11	1.52	2.10	0.44

TABLE V
Summary of Simulations for the Anode Mesh Model at $R_c = 3.8$ cm

A (%)	I_c (kA)	I_{dt} (kA)	ε_f (%)	ε_s (%)	ε_{sh} (%)	ε_l (%)	$\varepsilon_f/\varepsilon_l$
0	38.6	38.6	1.92	1.23	1.58	1.38	1.39
10	42.8	38.5	2.24	1.86	2.05	2.07	1.09
20	45.1	36.1	2.21	1.84	2.02	1.94	1.14
30	46.3	32.4	1.40	1.59	1.50	1.50	0.93
40	46.8	28.1	1.62	1.50	1.56	1.45	1.12

From the last column of Table IV a tendency toward a decrease of the ratio ϵ_f/ϵ_l with the increase in A is evident. The inequality $\epsilon_f > \epsilon_l$ keeps only for $A = 5\%$ and $A = 10\%$. For $A = 15\%$ and $A = 20\%$, $\epsilon_f \approx \epsilon_l$, while ϵ_f is considerably lower than ϵ_l if $A = 40\%$. The reason for such a behavior of ϵ_f is the following. At greater A, fewer electrons are involved in the bunching process (as a result of a mesh absorption) and E_z increases more slowly. Hence the microwave power and the efficiency calculated for the beginning of the pulse flat top are lower. For all investigated A values $\epsilon_{sh} \approx \epsilon_l$ (with the exception of the case $A = 40\%$). The largest values of the microwave radiation power, for $R_c = 3.4$ cm, were calculated for $\tau_{ft} = 0.6$ ns at $A = 5\%$ ($P \approx 135$ MW) and at $A = 10\%$ ($P \approx 150$ MW). These calculations were performed using the relation $P = \epsilon_f U I_{dt}$, where ϵ_f and I_{dt} are taken from Table IV.

Similar conclusions about the efficiencies are valid for $R_c = 3.8$ cm (see Table V). However, in this case $\epsilon_f > \epsilon_l$ until $A = 20\%$, which is an advantage in comparison with the previous case ($R_c = 3.4$ cm). An approximate equality between ϵ_f and ϵ_l occurs for $A = 30\%$. Surprisingly, when the probability of absorption reaches 40%, ϵ_f becomes higher than ϵ_l again. Nevertheless, the calculated mean microwave radiation power P at $\tau_{ft} = 0.6$ ns for $A = 40\%$ is $\approx$137 MW, which is considerably lower than $P \approx 240$ MW for $A = 20\%$ or $P \approx 260$ MW for $A = 10\%$.

From Tables IV and V it is seen that $\epsilon_f > \epsilon_s$ for $A \leq 20\%$. If $R_c = 3.8$ cm and $A = 40\%$ (see the last row of Table V), then ϵ_f is a little larger than ϵ_s. Consequently, for both cathode radii ($R_c = 3.4$ cm and $R_c = 3.8$ cm) it is reasonable to make efforts leading to shortening of τ_{ft} below 1.2 ns only when $A \leq 20\%$.

V. Conclusion

In this paper we have presented numerical simulation results carried out for the future experiments of a high-power virtual-

cathode reflex triode driven by an electron gun, designed and constructed at ENEA (Italy). The gun is able to produce repetitive short pulses, trapezoidal in shape with a full width and a flat top duration τ_{ft} of $\approx$3 ns and $\approx$1.2 ns, respectively. Some of the simulation parameters were fixed—the TEM pulse flat top voltage (300 kV) and the cathode–anode mesh distance (6 mm), while others were varied—the cathode radius R_c and the probability of absorption A.

The simulations performed show that at larger R_c ($\geq$ 2.8 cm) the efficiencies ϵ_{sh}, calculated for $\tau_{ft} = 1.2$ ns, are approximately equal to those determined for $\tau_{ft} = 4$ ns (1.5–2.1%). It must be noted that the R_c enlargement from 1.6 to 3.8 cm results in: first, ϵ_{sh} increase of about two times, and second, fourfold efficiency increase at fixed $\tau_{ft} = 0.6$ ns. On the other hand, for larger R_c, τ_{ft} shortening from 1.2 to 0.6 ns leads to a 10–15% efficiency enhancement, which occurs, however, at high transparency q of the anode mesh (80–90%). Hence, future changes of the ENEA gun construction resulting in τ_{ft} decrease below 1.2 ns are reasonable only for greater cathode radii and at small probability of absorption values ($\leq$20%). The maximum output microwave power (above 200 MW) was calculated for $R_c = 3.8$ cm at $\tau_{ft} = 0.6$ ns and at $A = 10\%$ and $A = 20\%$.

A shortening of the pulse flat top at constant rise and fall time leads to the appearance of three competing factors, as two of them are positive: 1) An increase of the efficiency (calculated for the flat top), which is evident from the simulations performed and is equivalent to a peak microwave power enhancement. 2) Increase of the mesh lifetime. This gives a possibility for a pulse repetition frequency rise. The negative factor consists of a reduction of the efficiency, calculated for the whole pulse, since the ratio of the flat top duration to the pulse duration drops.

It is interesting to investigate experimentally the optimal flat top duration with respect to the emitted microwave energy.

ACKNOWLEDGMENT

The authors thank V. Tarakanov for many useful discussions.

REFERENCES

[1] P. Raimondi and G. Messina, "High gradient linac for compact FEL," *Nucl. Instr. Meth. Phys. Res.*, vol. A358, pp. ABS34–ABS35, 1995.
[2] V. Tarakanov, *User's Manual for Code KARAT.* BRA, Inc., 1992.
[3] L. E. Thode, "Virtual-cathode microwave device research: experiment and simulation," in *High-Power Microwave Sources*, V. L. Granatstein and I. Alexeff, Eds. Norwood, MA: Artech, 1987, pp. 507–562.
[4] A. L. Peratt, C. M. Snell, and L. E. Thode, "A high-power reflex triode microwave source," *IEEE Trans. Plasma Sci.*, vol. PS-13, pp. 498–505, 1985.
[5] J. Benford and J. Swegle, *High-Power Microwaves.* Norwood, MA: Artech, 1992, pp. 307–337.
[6] H. A. Davis, R. R. Bartch, L. E. Thode, E. G. Sherwood, and R. M. Stringfield, "High-power microwave generation from a virtual cathode device," *Phys. Rev. Lett.*, vol. 55, pp. 2293–2296, 1985.
[7] R. A. Mahaffey, P. Sprangle, J. Golden, and C. A. Kapetanakos, "High-power microwaves from a nonisochronic reflecting electron system," *Phys. Rev. Lett.*, vol. 39, pp. 843–846, 1977.
[8] S. C. Burkhart, R. D. Scarpetti, and R. L. Lundberg, "A virtual-cathode reflex triode for high-power microwave generation," *J. Appl. Phys.*, vol. 58, pp. 28–36, 1985.

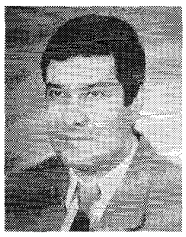

Ivailo G. Yovchev was born in Dimitrovgrad, Bulgaria, in 1958. In 1983, he graduated from Sofia University, Bulgaria, where he is currently working toward the Ph.D. degree.

Since 1984, he has worked as an Assistant Professor at the Higher Institute of Chemical Technology, Sofia, Bulgaria. In 1988, he joined in the investigations at the Plasma Electronics Laboratory, Sofia University. His research interests include beam dynamics and high-power microwave generation.

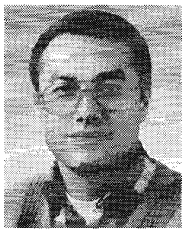

Ivan P. Spassovsky received the Ph.D. degree in physics from Sofia University, Sofia, Bulgaria.

From 1992 to 1993, he worked at the National Institute of Space Research-SP, Brazil, on the development and construction of the 35-GHz gyrotron. He moved to ENEA (Frascati, Italy) in 1994, where he joined the Free Electron Laser Team to work on the far-infrared FEL program and on the construction of the high-current electron gun for FEL driving. Since November 1995, he has been with the Laboratory of Quantum Optics at the Korean Atomic Research Institute–FEL Group. His current interests include high-current and RF accelerators, electron beams, and high-power microwaves.

Nikolai A. Nikolov was born in 1933 in Svistov, Bulgaria. He received the M.Sc. and Ph.D. degrees in physics from Sofia University, Sofia, Bulgaria, in 1957 and from Moscow State University, Russia, in 1972, respectively, and the D.Sc. degree in plasma physics in 1992 from Sofia University.

He has been an Associate Professor since 1977 and a full Professor since 1994 at Sofia University. He is the Head of the Plasma Electronics Laboratory at Sofia University, and since 1993, he has been the Dean of the Faculty of Physics. His research interests are in the resonance properties of magnetically confined plasma, beam dynamics, and high-power microwave generation.

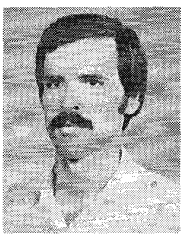

Dimitar P. Dimitrov was born in Cherni Vit, Bulgaria, in 1960. In 1985, he graduated from Sofia University, Sofia, Bulgaria, where is currently working toward the Ph.D. degree.

Since 1985, he has worked as a Researcher at the University of Mining and Geology, Sofia, Bulgaria. In 1993, he joined in the research works at the Plasma Electronics Laboratory, Sofia University. His scientific interests are in beam dynamics and high-power microwave generation.

Giovanni Messina was born in Trapani, Italy, on May 4, 1958. He received the Ph.D. degree in physics from Pisa University, Italy, in 1973.

After some experiences with the Quantum Electronics Team of the Physics Department of Pisa University, especially in the field of data acquisition for two photon spectroscopy experiments, in June 1979, he obtained a permanent position at the ENEA-Frascati Research Centre, Italy, where he is presently working in the Laser and Accelerator Division. His current scientific interests include some applications of electron accelerators, including generation of infrared and submillimeter waves in microtron-based free electron lasers and material processing using an electron beam produced by a 5-MeV linac.

Pantaleo Raimondi, photograph and biography not available at the time of publication.

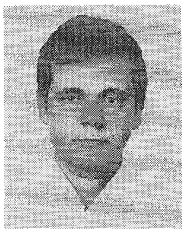

Joaquim J. Barroso received the B.S. degree in electrical engineering and the M.S. degree in plasma physics, both from the Technological Institute of Aeronautics, Brazil, in 1976 and 1980, respectively. In 1988, he received the Dr. degree in plasma physics from the Instituto Nacional de Pesquisas Espaciais (INPE), São Paulo, Brazil.

Since 1982, he has been with INPE where he has been involved in the design and construction of a high-power 32-GHz gyrotron. During 1989–1990, he was a Visiting Scientist at the Plasma Fusion Center of the Massachusetts Institute of Technology, Cambridge. His current research interests include high-power microwave generators and plasma technology.

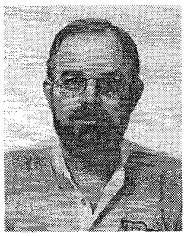

Rafael A. Corrêa received the B.S. degree in physics from the Universidade of São Paulo, Brazil, in 1978, the M.S. degree from the Instituto Nacional de Pesquisas Espaciais (INPE), São Paulo, Brazil, in 1983, and the Dr. degree in plasma physics from the Instituto Tecnológico de Aeronáutica, Brazil, in 1993.

He has been with the INPE since 1979, and in 1982, he joined the Laboratório Associado de Plasma of INPE. During 1994–1995, he was a Visiting Scientist at the Laboratory for Plasma Research, University of Maryland, College Park. His research interests are in gyrotrons, free electron lasers, and plasma physics.